Inorganic Chemistry

Article

pubs.acs.org/IC

Prion Peptides Are Extremely Sensitive to Copper Induced Oxidative Stress

Simone Dell'Acqua,[†] Chiara Bacchella,[†] Enrico Monzani,[†] Stefania Nicolis,[†] Giuseppe Di Natale,[‡] Enrico Rizzarelli,[‡] and Luigi Casella*[,†]

[†]Dipartimento di Chimica, Università di Pavia, Via Taramelli 12, 27100 Pavia, Italy

[‡]Istituto di Biostrutture e Bioimmagini, Consiglio Nazionale delle Ricerche, Via P. Gaifami 18, Catania, Italy

Supporting Information

ABSTRACT: Copper(II) binding to prion peptides does not prevent Cu redox cycling and formation of reactive oxygen species (ROS) in the presence of reducing agents. The toxic effects of these species are exacerbated in the presence of catecholamines, indicating that dysfunction of catecholamine vesicular sequestration or recovery after synaptic release is a dangerous amplifier of Cu induced oxidative stress. Cu bound to prion peptides including the high affinity site involving histidines adjacent to the octarepeats exhibits marked catalytic activity toward dopamine and 4-methylcatechol. The resulting quinone oxidation products undergo parallel oligomerization and endogenous peptide modification yielding catechol adducts at the histidine binding ligands. These modifications add to the more common oxidation of Met and His residues produced by ROS. Derivatization of Cu-prion peptides is much faster than that undergone by Cu-β-amyloid and Cu-α-synuclein complexes in the same conditions.

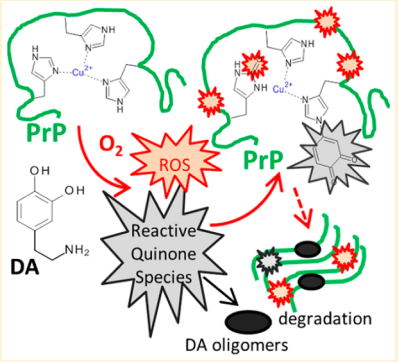

INTRODUCTION

The cellular prion protein (PrP) is a membrane-anchored glycoprotein of still incompletely understood physiological role, reaching high levels in the nervous system, and capable of producing a misfolded isoform, the prion, identified as the causative agent of several neurodegenerative diseases.[1] The infectious nature of the toxic isoform involves conformational remodeling and aggregation of PrP in a template-directed process.[2] Although human prion diseases are rare, the pathogenic mechanisms in much more common neurodegenerative diseases, such as Parkinson and Alzheimer's disease, appear to be similar to prions.[3] Therefore, both tau,[4] α-synuclein,[5] and β-amyloid[6] can undergo the same type of template conformational change as prions and then spread from cells to cells, at least within the brain.

The role of PrP has been often associated with its Cu binding properties, with affinity in the nanomolar range, or even lower,[7] but the unique feature of this protein is its ability to bind up to six Cu^{2+} ions, depending on the Cu^{2+} concentration. Copper plays an emerging role as a modulator of signal transduction, and its release at synapses can modulate neurotransmitter receptors.[8] In fact, Cu-PrP binding appears to modulate NMDA receptor activity,[9] attenuating glutamate excitotoxicity.[10] Interestingly, β-amyloid oligomers have been found to induce neurotoxicity by blocking Cu-PrP activity on the NMDA receptor, probably through Cu^{2+} chelation.[9] Recent findings describe the truncated β-amyloid (4−42) as mostly responsible for Cu^{2+} binding, due to its high affinity.[11] In general, PrP appears to play a central role in neuroprotection, and Cu-PrP complexes may be involved in cellular protection against oxidative stress.[12,13] The proposal that Cu-PrP exerts superoxide dismutase activity[14] has been challenged by subsequent studies.[15] However, high levels of oxidized methionines have been observed in prions,[16] and Cu-PrP was found to exert neuron protection through S-nitrosylation.[17] Therefore, there is an urgent need to shed light upon the potential reactivity of Cu-PrP under oxidative stress conditions and what are the consequences of this reactivity on the integrity of PrP protein.

In this paper, we focused on the redox reactivity of Cu^{2+} bound to three N-acetylated and C-amidated PrP fragments, $PrP_{106-114}$, PrP_{84-114}, and PrP_{76-114}. These span the region where binding of PrP by β-amyloid oligomers occurs,[18] which is key for the toxicity associated with Alzheimer's disease and include the fragment outside the octarepeats (92−114),[19] with the high affinity Cu site involving H96 and H111, and the larger fragments also containing one (84−114) or two (76−114) of the Cu sites within the four octarepeats.[20] Considering the complex pattern of Cu-PrP complexes that can be formed in various conditions,[19] we focused on Cu-PrP fragments at low Cu loading in physiological conditions. The structure of the main Cu species is given in Chart 1. As reactive molecules capable of inducing Cu redox cycling, we studied the neurotransmitter dopamine (DA) and the related, but structurally simpler, 4-methylcatechol (MC). Actually, a role of DA in promoting PrP aggregation,[21a] dimerization, and oxidative cleavage has been proposed.[21b] In addition, the

Received: July 10, 2017
Published: August 28, 2017

DOI: 10.1021/acs.inorgchem.7b01757
Inorg. Chem. 2017, 56, 11317−11325

Chart 1. Schematic Structures of the Main Species for Cu-PrP Peptides in a 1:1 Ratio at Physiological pH (A, B, and C, for Cu^{2+}, and D for Cu^{+})

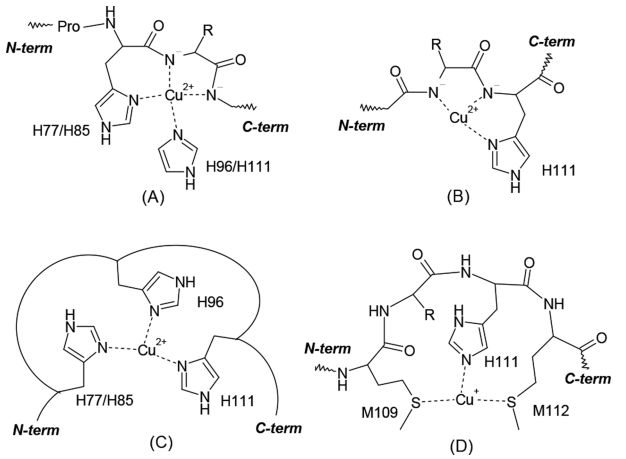

present investigation extends our comparative studies on the redox activity of Cu complexes with neuronal peptide fragments of β-amyloid[22] and α-synuclein.[23]

Structure A represents the main species for Cu^{2+} binding to PrP_{76-114} and PrP_{84-114} as deduced from potentiometric and spectroscopic studies.[19,20] Cu^{2+} is bound to an octarepeat fragment (75−81 or 83−89), with a contribution by an additional distal His. Structure B is the main species for Cu^{2+}-$PrP_{106-114}$;[19,20] note that H111 is outside the octarepeats; another ligand, that may be water, occupies the fourth coordination position. Structure C represents a hypothesized poly-His macrochelate complex involving Cu^{2+} binding to three or four His,[19] and this is a minor species at neutral pH but is appreciable at slightly acidic pH. Structure D shows the reduced Cu^{+}-PrP species, as deduced from spectroscopic and theoretical studies;[29b] it involves Met residues and H111 outside the octarepeats; also in this case a fourth donor ligand may be present.

RESULTS AND DISCUSSION

Oxidation of Dopamine and 4-Methylcatechol by Cu-PrP Complexes. As shown by the plots of Figures 1 and 2, the rate of oxidation of DA (3 mM) by air oxygen and Cu^{2+} (25 μM), in Hepes buffer at pH 7.4, is strongly promoted by

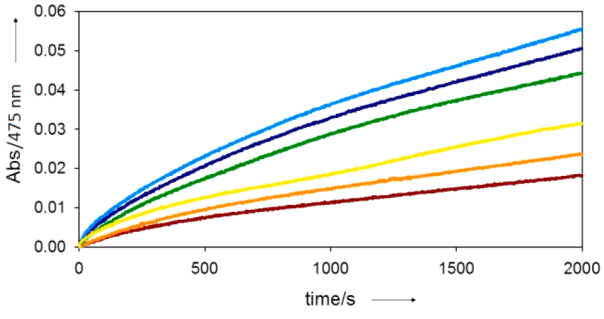

Figure 1. Kinetic profiles of DA (3 mM) oxidation with time (DA autoxidation in brown), in 50 mM Hepes buffer solution at pH 7.4 and 20 °C in the presence of Cu^{2+} (25 μM) (orange) and with addition of PrP_{76-114} (6 μM, yellow; 25 μM, green; 50 μM, blue; 75 μM, light blue). DA oxidation was monitored through the absorption band of dopaminochrome at 475 nm.

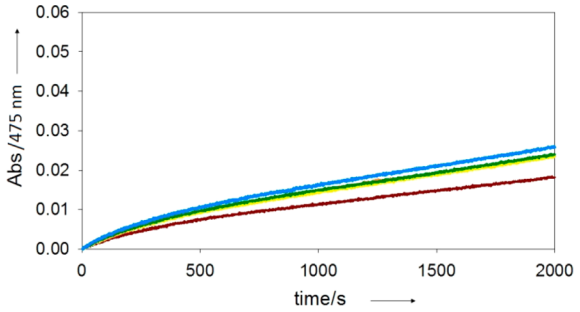

Figure 2. Kinetic profiles of DA (3 mM) oxidation with time (DA autoxidation in brown), in 50 mM Hepes buffer solution at pH 7.4 and 20 °C in the presence of Cu^{2+} (25 μM) (orange) and with addition of $PrP_{106-114}$ (25 μM, yellow; 50 μM, green; 75 μM, blue). DA oxidation was monitored through the absorption band of dopaminochrome at 475 nm.

increasing amounts of PrP_{76-114}; on the contrary, the effect of $PrP_{106-114}$ is very low. The behavior of PrP_{84-114} is more similar to that of PrP_{76-114} but DA oxidation is appreciably lower (see Figure S1). It should be noted that the optical traces at 475 nm monitor the dopaminochrome intermediate (see Scheme 1),[24] but DA oxidation gives rise to a complex mixture of products, as shown by the broad absorption bands in the spectra of the reaction mixture (see Figure S2).

Scheme 1. Initial Steps of the Dopamine Oxidation Pathway[a]

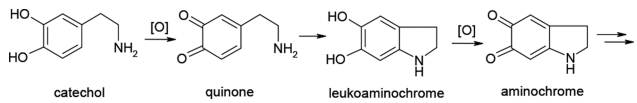

[a]The dopaminochrome intermediate is that with longer life and responsible for the broad absorption band between 450 and 500 nm. It undergoes further condensation and oxidative oligomerization reactions to produce insoluble melanic pigments.[24]

On the basis of previous thermodynamic studies,[19,25] it is possible to estimate the species distribution for the Cu-peptide complexes. The data obtained for Cu-PrP_{76-114} show that Cu^{2+} is fully complexed (99.4%) by the peptide already at a 1:1 ratio (see Table S1 and Figure S3). For Cu-PrP_{84-114} the situation is similar, with 93% Cu bound at a 1:1 Cu/peptide ratio (see Table S2 and Figure S4), whereas for Cu-$PrP_{106-114}$ at a 1:1 ratio a significant Cu fraction is bound to the buffer, and only at a 1:3 ratio most of Cu^{2+} is bound to the peptide (see Table S3 and Figure S5). For this reason, and also to take into account that oxidation experiments are carried out in the presence of more than 100 molar excess of catechol substrates, which are chelating ligands for Cu^{2+}, the kinetic traces were followed at increasing peptide/Cu^{2+} ratios, to ensure that conditions of full occupancy of the peptide are approached. In any case, the trend displayed in DA oxidation by the complexes clearly indicates the reactivity order: Cu-PrP_{76-114} ≥ Cu-PrP_{84-114} ≫ Cu-$PrP_{106-114}$.

A less discriminating behavior was observed in the oxidation of MC catalyzed by Cu-PrP peptides. This substrate has lower semiquinone/catechol redox potential and, lacking the amino group in the substituent chain, forms a more stable quinone with respect to DA.[23a] The $E^{\circ\prime}$ data for DA and MC redox couples are 0.53[26a] and 0.46 V,[26b] respectively, and should be compared with those of the Cu(II)/Cu(I) couples of Cu-PrP

DOI: 10.1021/acs.inorgchem.7b01757
Inorg. Chem. 2017, 56, 11317−11325

complexes. Here the literature values are more variable, ranging from 0.3 V, for the full length protein[27] to 0.57 V for PrP fragments including Met residues.[15c] It should be pointed out, however, that the species ruling the reaction is not the copper(II)-PrP complex but the intermediate [Cu-PrP-catechol-O_2], as discussed below.

The kinetic profiles of MC (3 mM) oxidation by Cu^{2+} (25 μM), in a time interval where 4-methylquinone is the only product,[22b] show a progressive increase of the rate with increasing equivalents of PrP_{76-114} (Figure 3). The rate increase

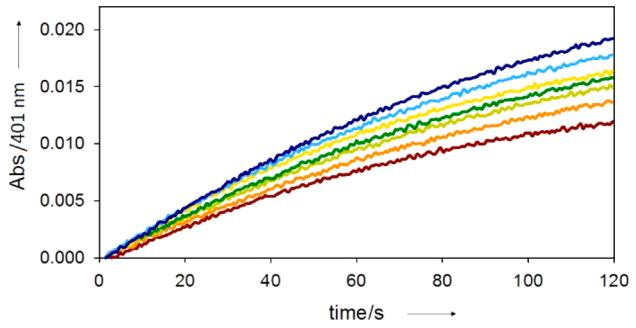

Figure 3. Kinetic profiles of MC (3 mM) oxidation with time, in 50 mM Hepes buffer solution at pH 7.4 and 20 °C in the presence of Cu^{2+} (25 μM) (brown) and with addition of PrP_{76-114} (10 μM, orange; 20 μM, light green; 25 μM, green; 35 μM, yellow; 50 μM, light blue; 75 μM, blue).

of MC oxidation promoted by PrP_{84-114} (Figure S6) and $PrP_{106-114}$ is similar (Figure S7). It is interesting to note that the promoting effect by PrP peptides on Cu reactivity resembles that of β-amyloid,[22b] whereas *N*-acetylated α-synuclein quenches Cu reactivity.[23]

As already characterized in a previous study,[23b] at longer reaction time the maximum absorption band shifts to 480 nm upon formation of an adduct between excess MC and the quinone. In the presence of free copper the addition product is the main species even after 90 min reaction time (Figures S8 and S9A), whereas in the presence of the Cu-PrP complex the reaction leads to further oligomeric products, as shown by the broadening of absorption between 400 and 800 nm (Figure S9B).

The reaction mechanism previously proposed for the oxidation of catechols by Cu-β-amyloid[22b] and Cu-α-synuclein[28] peptide complexes can be extended to the present Cu-PrP peptides. It involves the following reaction steps:

$$Cu^{2+} + PrP \rightleftarrows [Cu^{2+}\text{-}PrP] \quad (1)$$

$$[Cu^{2+}\text{-}PrP] + \text{catechol} \rightarrow [Cu^{+}\text{-}PrP] + \text{semiquinone}^{\bullet+} \quad (2)$$

$$[Cu^{+}\text{-}PrP] + \text{catechol} \rightleftarrows [Cu^{+}\text{-}PrP\text{-catechol}] \quad (3)$$

$$[Cu^{+}\text{-}PrP\text{-catechol}] + O_2 \rightarrow [\text{Cu-PrP-catechol-}O_2] \quad (4)$$

$$[\text{Cu-PrP-catechol-}O_2] \rightarrow\rightarrow [Cu^{2+}\text{-}PrP] + \text{quinone} \quad (5)$$

$$2\text{-semiquinone}^{\bullet+} \rightarrow \text{catechol} + \text{quinone} \quad (6)$$

The rate-determining step of the mechanism outlined by reactions 1−5 is reaction 4 of the reduced form of Cu-PrP peptides with dioxygen, to generate the ternary complex indicated as [Cu-PrP-catechol-O_2]. This was probed performing the MC oxidation experiment by Cu-PrP_{76-114} in a buffer solution saturated with pure oxygen (1 atm). The reaction rate indeed markedly increases with the increase of dioxygen concentration (Figure S10), showing that it is Cu^{+}, rather than Cu^{2+}, the species controlling the efficiency of the whole process. The reaction rate depends also on catechol concentration, with a hyperbolic behavior (Figure S11), indicating that substrate binding occurs as a pre-equilibrium step before the rate-determining binding of molecular oxygen. This shows that O_2 binds to the [Cu^{+}-PrP-catechol] adduct rather than [Cu^{+}-PrP].

The structure of the Cu^{+} species bound to PrP peptides was recently characterized with various techniques indicating that under physiological conditions the ligands are provided by the two Met residues and H111.[29b] However, upon redox cycling it is unlikely that Cu will undergo the structural changes corresponding to the more stable, resting Cu^{2+} and Cu^{+} forms (Chart 1), because this would involve large reorganization energy of the complex. The catalytically active form of Cu-PrP peptides 76−114 and 84−114 may correspond to the Tris-histidine environment shown in structure C of Chart 1, involving H96 and H111 outside the octarepeats, which should be accessible to both Cu^{2+} and Cu^{+} species. The third histidine is one contained in the octarepeats, His85 for PrP_{84-114} and either His85 or His77 for PrP_{76-114}.[19c] In the case of Cu-$PrP_{106-114}$ the situation must be obviously different, and the coordination set of the redox cycling copper can only correspond to structure D of Chart 1. Binding to the methionines stabilizes Cu(I) and clearly reduces its reactivity to O_2 and the catalytic activity of this Cu-PrP complex. Binding of the catechol to copper(I) may also affect the coordinative environment of the metal ion.

A similar situation where the proposed redox cycling Cu active species is different from the resting form of the Cu complexes was recently proposed for Cu-β-amyloid.[30] In the present case, a clear advantage in catalytic efficiency would be associated with the reduced $CuHis_3^{+}$ form, whose coordination set resembles the typical structural motif present in many copper enzymes activating dioxygen.[31]

We should also mention that an alternative pathway, operative for catechol oxidation promoted by free Cu^{2+}, can in principle occur competitively, to some extent, for the Cu-PrP complexes. This mechanism involves superoxide and hydroxyl radicals formed through the Fenton reaction:

$$Cu^{2+} + \text{catechol} \rightarrow Cu^{+} + \text{semiquinone}^{\bullet+} \quad (7)$$

$$Cu^{+} + O_2 \rightarrow Cu^{2+} + O_2^{-} \quad (8)$$

$$2O_2^{-} + 2H^{+} \rightarrow O_2 + H_2O_2 \quad (9)$$

$$H_2O_2 + Cu^{+} \rightarrow OH^{-} + OH^{\bullet} + Cu^{2+} \quad (10)$$

DOI: 10.1021/acs.inorgchem.7b01757
Inorg. Chem. 2017, 56, 11317−11325

An indication of the relative importance of this mechanism for the catechol oxidation by Cu-PrP complexes could be obtained through the assay of hydrogen peroxide in the reaction solution, because this is the slowly reacting species and can accumulate. Thus, when assayed in parallel experiments, the amount of H_2O_2, detected by a peroxidase assay after quenching the oxidation of MC after 10 min, was 2.8 mol % with respect to initial MC for Cu^{2+} and 1.7 mol % for Cu-PrP_{76-114} complex. It should be noted that the amount of hydrogen peroxide detected in the reaction of "free" Cu^{2+} is comparable to the MC oxidized after the same time (see Figure 5 below). On the other hand, accumulated H_2O_2 is only about 10% of the amount of MC oxidized with Cu-PrP_{76-114}.

We have also found that hydrogen peroxide can participate in catechol oxidation promoting a further, albeit less efficient, mechanism. As shown in Figure S12, addition of hydrogen peroxide to a solution of MC and copper(II) gives rise to an increase in the reaction rate, and the effect is larger in the presence of PrP_{76-114}. Therefore, the low accumulation of H_2O_2 observed for Cu-PrP_{76-114} is partly due to the better capacity of this complex to use the peroxide as an oxidant.

Competitive Endogenous PrP Peptide Oxidation. In a system which is not preorganized for dioxygen activation and contains kinetically labile copper, the intermediate Cu/O_2 species typically evolves through a Fenton reaction producing harmful ROS species (H_2O_2 and $OH^{\bullet}$), capable of performing nonselective oxidations. The reactivity of these species can be directed in particular toward the peptide, that can explain the protecting, albeit suicidal, role exerted by PrP and β-amyloid.[22] The presence of catecholic neurotransmitters further complicates the pattern of reactions occurring in the system, because their quinone oxidation products bear potential reactivity against nucleophilic amino acid side chains, as we have recently shown for α-synuclein[23a] and β-amyloid peptides.[22b] We have therefore investigated the possible competition between catechol oxidation and endogenous PrP peptide modification. DA is not the ideal catechol for these experiments, because its oxidative polymerization gives rise to a complex mixture of oligomeric, and intractable, products. The competition between catechol oxidation and peptide modification was therefore investigated using MC.

In these experiments, solutions of copper (25 μM) and PrP peptides (25 μM) were incubated in the presence of MC (3 mM), and the mixture was analyzed by LC/MS at different reaction times. The MS/MS spectra of the ion series obtained upon peptide fragmentation allow identifying the modification sites. The data show that all PrP peptides undergo severe modification upon Cu redox cycling, even at relatively short reaction times, in spite of the presence of more than 100 molar excess of catechol. For instance, in the case of PrP_{76-114}, 14% peptide underwent modification after 10 min reaction time and almost 30% after 35 min (Table 1 and Figure 4). The main modifications correspond to (i) oxidation (+16 Da mass increment) of one of the histidines in the octarepeat region (H77, H85) or the external H96 (R_t 32′), and one of the two methionines (M109, M112) or, less likely, H111 (R_t 29′); (ii) the formation of a covalent adduct (+120 Da) between one His residue outside the octarepeat region (H96, H111) and 4-methylquinone (MQ) (Scheme S1); (iii) oxidation of one octarepeat His in addition to the former His(96/111)-MQ adduct (+136 Da); and (iv) formation of two His-MQ adducts at H96 and H77/H85, and oxidation of the other octarepeat His (H85/H77) (+256 Da). These derivatizations are worth noting considering that they occur at His residues we propose as the copper binding ligands for the redox cycling Cu-PrP_{76-114} species or at Met residues close to them (Chart 1).

Table 1. Modifications of PrP_{76-114} Detected by LC/MS Analysis, upon Oxidation of MC (3 mM) by Cu-PrP_{76-114} (25 μM) in 50 mM Hepes Buffer at pH 7.4 and 20 °C

peptide	Prp_{76-114} (%)	+16 His (%)	+16 Met (%)	+120 His (%)	+136 His (%)	+256 His (%)
time (min)	(R_t 30′)	(R_t 32′)	(R_t 29′)	(R_t 34′)	(R_t 33′)	(R_t 35′)
1	96.8	0.3	1.4	0.9	0.5	0.1
10	86.2	2.1	3.0	6.0	2.2	0.5
20	81.1	3.9	3.3	6.7	3.4	1.6
35	71.1	5.5	4.4	10.4	5.6	3.0
60	65.1	6.8	3.8	10.8	8.6	4.9
90	20.3	16.9	4.0	12.5	27.1	19.2
110	17.7	17.5	6.9	15.0	27.0	15.9

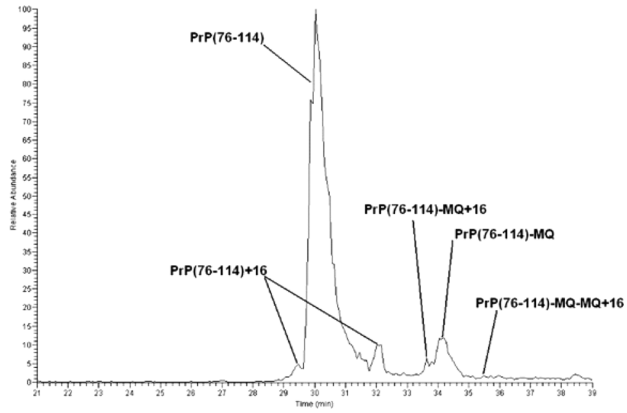

Figure 4. HPLC-MS elution profile of peptides produced upon oxidation of MC (3 mM) by Cu-PrP_{76-114} (25 μM) after 35 min reaction time in 50 mM Hepes buffer at pH 7.4 and 20 °C. The assignment of the peaks is given, with MQ indicating a mass increment of 120 Da and corresponding to the formation of a covalent adduct of the peptide with 4-methylquinone.

The pattern of modifications undergone by Cu-PrP_{84-114} in the same conditions is similar (Figure S13 and Table S4) and confirm the propensity of His and Met residues of PrP peptides to intercept ROS and in the first case reactive quinone species. The peptide modification pattern for $PrP_{106-114}$ shows more extensive oxidative damage at Met residues (see Figure S14 and Table S5), in agreement with the different structure of the redox cycling Cu(II)/Cu(I) species. In summary, the data from the competitive peptide modification studies confirm the hypothesis on the structure of the catalytically active species of Cu-PrP complexes suggested previously.

It is important to analyze in more quantitative terms the competition between catechol oxidation and endogenous peptide modification processes. To this end, the reaction mixtures resulting from MC oxidation in the same conditions described above were analyzed by NMR spectroscopy, monitoring the decrease of MC concentration with time. The spectrum of the reaction mixture was recorded after 5 min and every 30 min reaction time, following, in parallel, MC oxidation by Cu^{2+} and Cu^{2+}-PrP_{76-114} (Figure 5). The decrease in intensity of the MC signal at 6.55−6.75 ppm was used to monitor the progress of the reaction, with the Hepes buffer signal at 3.7 ppm serving as an internal standard (Figure S15).

DOI: 10.1021/acs.inorgchem.7b01757
Inorg. Chem. 2017, 56, 11317−11325

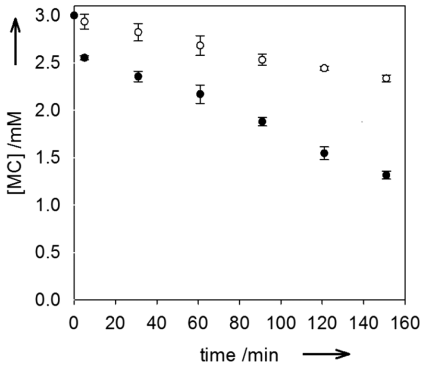

Figure 5. Consumption of MC (3 mM) evaluated by NMR spectroscopy, in 5 mM Hepes deuterated buffer solution at pH 7.4 and 20 °C in the presence of Cu^{2+} (25 μM) (open circles) and Cu^{2+}-PrP_{76-114} (25 μM) (full circles).

Representative spectra (Figure S16) and numerical data on the decrease of MC concentration in solution with time (Table S6) are given in the Supporting Information.

It can be noted that the rate of MC consumption is higher in the initial phase and then decreases as the peptide modification becomes more significant. However, the results are in agreement with the kinetic plots shown in Figure 2 and Figure S8, showing that the presence of prion peptide increases the reactivity of copper(II) in the oxidation of MC (and much more so for DA, see Figure 1).

The data obtained in these experiments can be compared with those obtained in the HPLC-MS/MS analysis (Figure 4 and Table 1). After 90 min reaction time in the presence of Cu^{2+} and MC, 80% of PrP_{76-114} (20 μM) undergoes modification with concomitant consumption of 1.10 mM MC, indicating approximately a ratio of 1 molecule peptide modified every 50 molecules MC reacted. Therefore, even an easy to oxidize external substrate does not protect the peptide from oxidation. In addition, as a consistent fraction of peptide undergoes modification by MC/MQ residues, this indicates that part of the reactive species formed during catalysis promoted by copper has the endogenous peptide as target.

SOD-like Reactivity of Cu-PrP Complexes. We also measured the SOD-like activity of Cu^{2+}-PrP peptide complexes in comparison to the activity of free Cu^{2+} in solution. The activity was evaluated through the direct assay in which O_2^- is supplied as KO_2-crown ether complex, as we reported previously for Cu-β-amyloid[22a] and Cu-α-synuclein[23a] peptide complexes. As shown in Figure S17, neither PrP_{76-114}, nor PrP_{84-114} and $PrP_{106-114}$ increase the SOD activity of free Cu^{2+}, and this result supports the conclusions based on different SOD assays.[15]

CONCLUSIONS

We have shown that redox cycling of Cu-PrP complexes induced by reactive catechols, such as catecholamine neurotransmitters, produces a much more complex pattern of peptide modifications than that resulting from simple reduction/reoxidation of Cu in the presence of reducing agents, that has been studied so far.[29] This is important in view of the emerging role of copper as neurotransmission modulator,[32] and in particular its involvement in the control of neurotransmitter receptor activity.[9] The present results emphasize the need of a strict homeostatic control of copper upon its release and recycle within the synaptic cleft. This control cannot be based only on high affinity binding of Cu^{2+} to proteins and peptides. In fact, the induction of ROS and more extensive post-translational modifications upon interaction of Cu with catecholamines occur even though copper may be bound to β-amyloid[22b] or PrP. Although it is worth emphasizing that the type of oxidative modifications occurring in hours on Cu-β-amyloid takes only minutes in the case of Cu-PrP peptides in the same conditions. Apparently, only binding to *N*-acetylated α-synuclein[23] seems to be protective against the aberrant modifications produced on neuronal peptides as a result of Cu redox reactivity. Quinone modification, so far recognized to affect specific proteins involved in Parkinson's disease, such as α-synuclein[33] and parkin,[34] occurs easily on PrP peptides, and also on β-amyloid,[22b] and may represent a more general mechanism occurring in neurodegenerative diseases, as a result of Cu-induced oxidative stress. As a matter of fact, dopaminergic neuron loss has been very recently reported to occur in Alzheimer's disease patients in brain regions different from the *substantia nigra*, which typically affects Parkinsonian subjects.[35] The effects of DA induced ROS on PrP were previously recognized on neuronal cells,[21a] and Cu-loaded recombinant PrP_{23-231} (Cu_5-PrP).[21b] The treatment produced aggregation,[21a] and protein carbonyls and fragmentation of the protein.[21b] Other reports described ROS induced cleavage of PrP induced by copper(II) and reductants,[36] but in all these studies specific modifications were not investigated.

The (patho)physiological relevance of the interaction of DA (and more generally brain catecholamines), Cu and PrP is related to the simultaneous presence of the three partners upon extracellular DA release in glutamatergic synapses, particularly from degenerating DA neurons. Similar processes may be induced by other catecholamines. Simple protein/peptide modifications corresponding to the addition of a quinone molecule (or a few molecules) have not been identified (and probably have never been searched either) but are unlikely to be detected in the materials, e.g., amyloid deposits and plaques, obtained from diseased brains, because these materials contain derivatizations produced over very long time periods, typically several years, and therefore the initially formed peptide-quinone addition products will be further processed and oligomerized. However, the experimental signature of the involvement of quinone species derived from catecholamine neurotransmitters in protein modification is provided by neuromelanins, which are complex, insoluble substances consisting of covalently bound melanin, protein, and lipid components.[37] Neuromelanin granules, in fact, have been detected in all major brain regions.[38] The synapse clefts and glutamatergic terminals are then the plausible sites where neurotransmitters, metal ions, and amyloidogenic peptide fragments from APP and prion proteins can meet and interact.[39]

MATERIALS AND METHODS

Materials and Instrumentation. Protected amino acids, rink amide resin, and other reagents for peptide synthesis, were purchased from Novabiochem. All other chemicals were reagent grade from Sigma-Aldrich. Peptide purifications were performed on a Jasco HPLC instrument equipped with two PU-1580 pumps and a MD-1510 diode array detector (working range: 195−659 nm), using a Phenomenex Jupiter 4U Proteo semipreparative column (4 μm, 250 × 10 mm). Mass spectra and LC-MS/MS data were obtained with a LCQ ADV MAX ion-trap mass spectrometer, with an ESI ion source. The system was run in automated LC-MS/MS mode and using a surveyor HPLC system (Thermo Finnigan, San Jose, CA, USA) equipped with a Phenomenex Jupiter 4U Proteo column (4 μm, 150 × 2.0 mm). For

DOI: 10.1021/acs.inorgchem.7b01757
Inorg. Chem. 2017, 56, 11317−11325

the analysis of peptide fragments, Bioworks 3.1 and Xcalibur 2.0.7 SP1 software were used (Thermo Finnigan, San Jose, CA (USA)). UV−vis spectra and kinetic experiments were recorded on an Agilent 8453 diode array spectrophotometer, equipped with a thermostated, magnetically stirred optical cell. NMR spectra were recorded on a Bruker AVANCE 400 spectrometer.

Peptide Synthesis. The two peptides PrP_{84-114} (Ac-PHGGGW-GQGGGTHSQWNKPSKPKTNMKHMAG-NH_2, mw 3297.65) and PrP_{76-114} (Ac-PHGGGWGQPHGGWGQGGGTHSQWNK-PSKPKTNMKHMAG-NH_2, mw 4074.45) were synthesized according to literature procedures.[19a,b]

$Prp_{106-114}$ (Ac-KTNMKHMAG-NH_2, mw 1057.5) peptide was synthesized using the standard fluorenyl methoxycarbonyl (Fmoc) solid-phase synthesis in DMF. Rink-amide resin MBHA (substitution 0.64 mmol/g) was used as polymeric support, which yielded the peptide amidated at the C-terminus.

After deprotection of the resin by treating the support twice, for 3 and 7 min, with 20 mL of 20% (v:v) piperidine in DMF, the first amino acid (2 mol equiv vs. resin sites) was added in the presence of 2 equiv of *N*-hydroxybenzotriazole (HOBt), 2 equiv of benzotriazol-1-yl-oxytripyrrolidinophosphonium hexafluorophosphate (PyBOP), and ∼2 equiv of *N*,*N*-diisopropylethylamine (DIEA). After 45 min, the same coupling procedure was repeated. After recoupling of each amino acid, a capping step was performed by using 20 mL of 4.7% acetic anhydride and 4% of pyridine in DMF; resin was washed by DMF, dichloromethane, and isopropanol. At the end of the synthesis, the protections of the side chains of the amino acids were removed with a solution of 95% trifluoroacetic acid (TFA, 25 mL for 1 g of resin), triisopropyl silane (2.5%), and water (2.5%), which serves also to release the peptide from the resin. After stirring for 3 h, cold diethyl ether was added to precipitate the peptide and the mixture was filtered; then, it was dissolved in water and purified by HPLC, using a 0−100% linear gradient of 0.1% TFA in water to 0.1% TFA in CH_3CN over 40 min (flow rate of 3 mL/min, loop 2 mL), as eluent. $Prp_{106-114}$ showed a retention time of ∼21−22 min. The product was then lyophilized and stored at −30 °C until use. The identity of the peptide was confirmed by electrospray ionization mass spectrometry (Thermo-Finnigan). ESI-MS data (direct injection, MeOH, positive-ion mode, capillary temperature 200 °C): *m*/*z* 1058 ($PrP_{106-114}^{+}$), 530 ($PrP_{106-114}^{2+}$), 358 ($PrP_{106-114}^{3+}$).

Kinetics of Oxidation of Catecholic Substrates. *Dopamine Oxidation.* The catalytic oxidation of DA by Cu^{2+} was studied at 20 °C in 50 mM Hepes buffer at pH 7.4, saturated with atmospheric oxygen. The reaction was monitored by UV−visible spectroscopy through the absorption band of dopaminochrome at 475 nm. First, DA autoxidation experiment and kinetic profile of the reaction catalyzed by Cu^{2+} were evaluated; the effect of PrP peptides on the copper-catalyzed DA oxidation was studied by adding the peptide in variable stoichiometry (0−4 equiv vs Cu^{2+}) to the reaction solution. This experiments were carried out by adding copper(II) nitrate (25 μM) as the last reagent to the solution containing DA (3 mM) and prion peptide (25−75 μM). All measurements were performed in triplicate.

4-Methylcatechol Oxidation. The catalytic oxidation of MC by Cu^{2+} was studied at 20 °C in 50 mM Hepes buffer at pH 7.4, saturated with atmospheric oxygen. The reaction was monitored by UV−visible spectroscopy through the absorption band of 4-methylquinone at 401 nm (ε = 1550 M^{-1} cm^{-1}). Copper(II) nitrate (25 μM) and substrate (3 mM) were kept constant, and PrP peptides were added at 0−75 μM concentrations. All measurements were performed in triplicate. MC oxidation experiments were also performed under oxygen saturating conditions, obtained by bubbling extensively with dioxygen (1 atm) the buffer solution. The effect of substrate concentration was investigated by keeping constant the amounts of copper(II) (25 μM) and PrP (25 μM) and varying MC concentration from 0.15 to 4.0 mM.

Detection of Hydrogen Peroxide in the Catalytic Reactions. The detection of hydrogen peroxide during the catalytic reaction was carried out by a peroxidase assay, as previously described,[40] with some minor modifications. The development of the characteristic I_3^- band (λ_{max} 353 nm; ε = 26 000 M^{-1} cm^{-1}), upon reaction with I^-, was monitored. The oxidation reaction of MC in the presence of Cu^{2+} or Cu^{2+}-PrP_{76-114} complex was carried out as in the kinetic experiments. The reaction was quenched after 10 min with addition of H_2SO_4 to pH 2 and an equal volume of water was added. The quinone formed was extracted three times using dichloromethane (removal of the quinone is necessary since it can oxidize iodide). The water layer and one-half volume of a solution of KI (0.5 M) in water and horseradish peroxidase (about 200 nM) were added.

In the presence of hydrogen peroxide, a band due to the formation of I_3^- develops. Since atmospheric oxygen can oxidize I^-, blank experiments (without catalyst or without catechol) were also performed. For the catalytic reactions performed in the presence of Hepes buffer or MC alone, almost negligible H_2O_2 accumulation was found. Instead, when the reaction was performed in the presence of copper(II) salt or Cu^{2+}-PrP_{76-114} complex, the assay revealed a concentration hydrogen peroxide corresponding to 2.8% and 1.7% of the initial catechol concentration, respectively.

Effect of Hydrogen Peroxide on the Kinetics of MC Oxidation. In these experiments, the reactivity of free copper(II) (25 μM) in MC (3 mM) oxidation in the presence of hydrogen peroxide (1 mM) was compared to that of copper(II) (25 μM) and PrP_{76-114} (25 μM), in 50 mM Hepes buffer solution at pH 7.4 and 20 °C. The presence of H_2O_2 was found to increase slightly the rate of formation of MQ in both cases (Figure S12).

Identification and Characterization of Modified Peptides by HPLC-ESI/MS. The competitive peptide modification was studied by HPLC-ESI/MS, preparing samples in the presence of copper(II) nitrate (25 μM), PrP (25 μM), and MC (3 mM) in Hepes buffer (50 mM) pH 7.4. HPLC-ESI/MS analysis were performed at different reaction times. LC-MS data were obtained by using a LCQ ADV MAX ion-trap mass spectrometer. The elution of PrP_{84-114} and PrP_{76-114} was carried out by using 0.1% HCOOH in distilled water (solvent A) and 0.1% HCOOH in acetonitrile (solvent B), with a flow rate of 0.2 mL/min; elution started with 98% solvent A for 5 min followed by a linear gradient from 98 to 55% A in 65 min. The elution of $PrP_{106-114}$ was performed by using pure distilled water (solvent A) and 0.1% HCOOH in acetonitrile (solvent B).

Computed Species Distribution Diagrams of Copper(II)-PrP Peptide Complexes. The species distribution as a function of the pH was obtained using the computer program Hyss.[41]

Species distribution diagrams of copper(II)-PrP_{76-114}, copper(II)-PrP_{84-114}, and copper(II)-$PrP_{106-114}$ systems are calculated according to the stability constants reported in potentiometric studies.[19a,b,25] The overall stability constant refers to the following equilibrium:

$$pM + qL + rH = M_pL_qH_r$$

And is expressed by the equation:

$$\beta_{pqr} = \frac{[M_pL_qH_r]}{[M]^p \cdot [L]^q \cdot [H]^r}$$

where β_{pqr}, $[m_pl_qh_r]$, [M], [L], and [H] are the overall stability constants, the free concentrations of the complex, the metal ion, and the proton, respectively. Copper(II) hydrolysis constants and Cu-Hepes (Cu−B) stability constant are from refs 42 and43, respectively.

NMR Quantification of Oxidized Catechol. The consumption of MC was monitored recording proton NMR spectra of a solution containing Hepes buffer (5 mM) at pH 7.4 and MC (3 mM) in deuterium oxide at 20 °C. Integrated area of the peak at 3.7 ppm of Hepes buffer was used as internal standard for the determination of MC concentration, calculated from the area of the signal of proton C (Figure S14) at 6.55−6.60 ppm. The initial spectrum in the presence of Hepes and MC serves as time zero point of Table S6 and Figure 4. The acquisition was repeated after the addition of copper(II) nitrate (25 μM) and Cu^{2+}-PrP_{76-114} complex (25 μM). The initial data were obtained after 5 min, which is the time required to acquire the spectrum. The acquisition was repeated in the same conditions every 30 min until 150 min reaction time.

In order to overcome the low availability of dioxygen in the NMR tube, the reaction was carried out in an open vial and transferred to the

DOI: 10.1021/acs.inorgchem.7b01757
Inorg. Chem. 2017, 56, 11317−11325

NMR tube prior to each spectral recording. A blank experiment performed entirely in the NMR tube confirmed that the reaction rate of MC oxidation was much slower due to slow diffusion of dioxygen to replace its consumption in the solution.

Superoxide Dismutase Activity. The SOD-like activity of [Cu^{2+}-PrP] complex was compared to activity of free Cu^{2+} in solution. The activity was evaluated through the direct assay in which O_2^- is directly generated by dissolution of KO_2 salt (28 mM) in a solution of 18-crown-6 ether (80 mM) in anhydrous DMSO and detected by the reaction with nitro blue tetrazolium (NBT) (1.25 mM) in phosphate buffer, which forms methyl formazane (MF^+), characterized by an intense absorption band at 560 nm.[44] After sonication, the solution becomes light yellow. UV−visible readings were performed in 50 mM phosphate buffer at pH 7.4 with the following final concentrations: 0.2 mM NBT, variable amounts of copper(II) (0−10 μM) and [Cu^{2+}-PrP] complex (0−10 μM, with a 1:1 ratio of Cu/peptide), 0.4 mM KO_2 from the 18-crown-6 ether solution in DMSO. All measurements were performed in triplicate.

■ ASSOCIATED CONTENT

Supporting Information

The Supporting Information is available free of charge on the ACS Publications website at DOI: 10.1021/acs.inorgchem.7b01757.

Supporting figures, tables, kinetic experiments, copper-peptide species distributions, NMR and MS spectra, SOD activity experiments (PDF)

■ AUTHOR INFORMATION

Corresponding Author

*E-mail: luigi.casella@unipv.it.

ORCID

Enrico Rizzarelli: 0000-0001-5367-0823

Luigi Casella: 0000-0002-7671-0506

Notes

The authors declare no competing financial interest.

■ ACKNOWLEDGMENTS

The authors acknowledge the Italian Ministry of Education, University, and Research (MIUR) - Research Projects of National Interest (PRIN) 2015 prot. 2015T778JW. C.I.R.C.M.S.B. is also acknowledged.

■ REFERENCES

(1) (a) Prusiner, S. B. Biology and genetics of prions causing neurodegeneration. *Annu. Rev. Genet.* **2013**, *47*, 601−623. (b) Collinge, J. Mammalian prions and their wider relevance in neurodegenerative diseases. *Nature* **2016**, *539*, 217−226.

(2) Halliday, M.; Radford, H.; Mallucci, G. R. Prions: Generation and spread versus neurotoxicity. *J. Biol. Chem.* **2014**, *289*, 19862−19868.

(3) Prusiner, S. B. Cell biology. A unifying role for prions in neurodegenerative diseases. *Science* **2012**, *336*, 1511−1513.

(4) Frost, B.; Jacks, R. L.; Diamond, M. I. Propagation of tau misfolding from the outside to the inside of a cell. *J. Biol. Chem.* **2009**, *284*, 12845−12852.

(5) Desplats, P.; Lee, P. H.; Bae, E. J.; Patrick, C.; Rockenstein, E.; Crews, L.; Spencer, B.; Masliah, E.; Lee, S. J. Inclusion formation and neuronal cell death through neuron-to-neuron transmission of α-synuclein. *Proc. Natl. Acad. Sci. U. S. A.* **2009**, *106*, 13010−13015.

(6) Petkova, A. T.; Leapman, R. D.; Guo, Z.; Yau, W. M.; Matson, M. P.; Tycko, R. Self-propagating, molecular-level polymorphism in Alzheimer's beta-amyloid fibrils. *Science* **2005**, *307*, 262−265.

(7) (a) Stanyon, H. F.; Patel, K.; Begum, N.; Viles, J. H. Copper(II) Sequentially loads onto the N-terminal amino group of the cellular prion protein before the individual octarepeats. *Biochemistry* **2014**, *53*, 3934−3939. (b) Walter, E. D.; Stevens, D. J.; Spevacek, A. R.; Visconte, M. P.; Dei Rossi, A.; Millhauser, G. L. Copper binding extrinsic to the octarepeat region in the prion protein. *Curr. Protein Pept. Sci.* **2009**, *10*, 529−535. (c) Arena, G.; La Mendola, D.; Pappalardo, G.; Sovago, I.; Rizzarelli, E. Interactions of Cu^{2+} with prion family peptide fragments: Considerations on affinity, speciation and coordination. *Coord. Chem. Rev.* **2012**, *256*, 2202−2218.

(8) (a) Grubman, A.; White, A. R. Copper as a Key Regulator of Cell Signalling Pathways. *Expert Rev. Mol. Med.* **2014**, *16*, e11. (b) D'Ambrosi, N.; Rossi, L. Copper at synapse: Release, binding and modulation of neurotransmission. *Neurochem. Int.* **2015**, *90*, 36−45. (c) Chang, C. J. Bioinorganic lfe and neural activity: Toward a chemistry of consciousness? *Acc. Chem. Res.* **2017**, *50*, 535−538.

(9) You, H.; Tsutsui, S.; Hameed, S.; Kannanayakal, T. J.; Chen, L.; Xia, P.; Engbers, J. D. T.; Lipton, S. A.; Stys, P. K.; Zamponi, G. W. Aβ neurotoxicity depends on interactions between copper ions, prion protein, and N-methyl-D-aspartate receptors. *Proc. Natl. Acad. Sci. U. S. A.* **2012**, *109*, 1737−1742.

(10) Khosravani, H.; Zhang, Y.; Tsutsui, S.; Hameed, S.; Altier, C.; Hamid, J.; Chen, L.; Villemaire, M.; Ali, Z.; Jirik, F. R.; Zamponi, G. W. Prion protein attenuates excitotoxicity by inhibiting NMDA receptors. *J. Cell Biol.* **2008**, *181*, 551−565.

(11) (a) Mital, M.; Wezynfeld, N. E.; Frączyk, T.; Wiloch, M. Z.; Wawrzyniak, U. E.; Bonna, A.; Tumpach, C.; Barnham, K. J.; Haigh, C. L.; Bal, W.; Drew, S. C. A Functional role for Aβ in metal homeostasis? N-Truncation and high-affinity copper binding. *Angew. Chem., Int. Ed.* **2015**, *54*, 10460−10464. (b) Wezynfeld, N. E.; Stefaniak, E.; Stachucy, K.; Drozd, A.; Plonka, D.; Drew, S. C.; Krężel, A.; Bal, W. Resistance of Cu(Aβ4−16) to copper capture by metallothionein-3 supports a function for the Aβ4−42 peptide as a synaptic cuii scavenger. *Angew. Chem., Int. Ed.* **2016**, *55*, 8235−8238.

(12) Haigh, C. L.; Drew, S. C.; Boland, M. P.; Masters, C. L.; Barnham, K. J.; Lawson, V. A.; Collins, S. J. Dominant roles of the polybasic proline motif and copper in the PrP23−89-mediated stress protection response. *J. Cell Sci.* **2009**, *122*, 1518−1528.

(13) Nadal, R. C.; Abdelraheim, S. R.; Brazier, M. W.; Rigby, S. E. J.; Brown, D. R.; Viles, J. H. Prion protein does not redox-silence Cu^{2+}, but is a sacrificial quencher of hydroxyl radicals. *Free Radical Biol. Med.* **2007**, *42*, 79−89.

(14) (a) Brown, D. R.; Clive, C.; Haswell, S. J. Antioxidant activity related to copper binding of native prion protein. *J. Neurochem.* **2001**, *76*, 69−76. (b) Thackray, A. M.; Knight, R.; Haswell, S. J.; Bujdoso, R.; Brown, D. R. Metal imbalance and compromised antioxidant function are early changes in prion disease. *Biochem. J.* **2002**, *362*, 253−258.

(15) (a) Jones, S.; Batchelor, M.; Bhelt, D.; Clarke, A. R.; Collinge, J.; Jackson, G. S. Recombinant prion protein does not possess SOD-1 activity. *Biochem. J.* **2005**, *392*, 309−312. (b) La Mendola, D.; Bonomo, R. P.; Caminati, S.; Di Natale, G.; Emmi, S. S.; Hansson, O.; Maccarrone, G.; Pappalardo, G.; Pietropaolo, A.; Rizzarelli, E. Copper(II) complexes with an avian prion N-terminal region and their potential SOD-like activity. *J. Inorg. Biochem.* **2009**, *103*, 195−204. (c) Shearer, J.; Soh, P. The copper(II) adduct of the unstructured region of the amyloidogenic fragment derived from the human prion protein is redox-active at physiological pH. *Inorg. Chem.* **2007**, *46*, 710−719.

(16) Canello, T.; Engelstein, R.; Moshel, O.; Xanthopoulos, K.; Juanes, M. E.; Langeveld, J.; Sklaviadis, T.; Gasset, M.; Gabizon, R. Methionine sulfoxides on PrP^{sc}: A prion-specific covalent signature. *Biochemistry* **2008**, *47*, 8866−8873.

(17) Gasperini, L.; Meneghetti, E.; Pastore, B.; Benetti, F.; Legname, G. Prion protein and copper cooperatively protect neurons by modulating NMDA receptor through S-nitrosylation. *Antioxid. Redox Signaling* **2015**, *22*, 772−784.

(18) Fluharty, B. R.; Biasini, E.; Stravalaci, M.; Sclip, A.; Diomede, L.; Balducci, C.; La Vitola, P.; Messa, M.; Colombo, L.; Forloni, G.; Borsello, T.; Gobbi, M.; Harris, D. A. An N-terminal fragment of the prion protein binds to amyloid-β oligomers and inhibits their neurotoxicity in vivo. *J. Biol. Chem.* **2013**, *288*, 7857−7866.

DOI: 10.1021/acs.inorgchem.7b01757
Inorg. Chem. 2017, 56, 11317−11325

(19) (a) Osz, K.; Nagy, Z.; Pappalardo, G.; Di Natale, G.; Sanna, D.; Micera, G.; Rizzarelli, E.; Sóvágó, I. Copper(II) interaction with prion peptide fragments encompassing histidine residues within and outside the octarepeat domain: Speciation, stability constants and binding details. *Chem. - Eur. J.* **2007**, *13*, 7129−7143. (b) Di Natale, G.; Osz, K.; Nagy, Z.; Sanna, D.; Micera, G.; Pappalardo, G.; Sóvágó, I.; Rizzarell, E. Interaction of copper(II) with the prion peptide fragment huPrP(76−114) encompassing four histidyl residues within and outside the octarepeat domain. *Inorg. Chem.* **2009**, *48*, 4239−4250. (c) Di Natale, G.; Turi, I.; Pappalardo, G.; Sóvágó, I.; Rizzarelli, E. Cross-talk between the octarepeat domain and the fifth binding site of prion protein driven by the interaction of copper(II) with the N-terminus. *Chem. - Eur. J.* **2015**, *21*, 4071−4084.

(20) (a) Chattopadhyay, M.; Walter, E. D.; Newell, D. J.; Jackson, P. J.; Aronoff-Spencer, E.; Peisach, J.; Gerfen, G. J.; Bennett, B.; Antholine, W. E.; Millhauser, G. L. The Octarepeat Domain of the Prion Protein Binds Cu(II) with Three Distinct Coordination Modes at pH 7.4. *J. Am. Chem. Soc.* **2005**, *127*, 12647−12656. (b) Quintanar, L.; Rivillas-Acevedo, L.; Grande-Aztatzi, R.; Gomez-Castro, C. Z.; Arcos-Lopez, T.; Vela, A. Copper coordination to the prion protein: Insights from theoretical studies. *Coord. Chem. Rev.* **2013**, *257*, 429−444.

(21) (a) da Luz, M. H. M.; Peres, I. T.; dos Santos, T. G.; Martins, V. R.; Icimoto, M. Y.; Lee, K. S. Dopamine induces the accumulation of insoluble prion protein and affects autophagic flux. *Front. Cell. Neurosci.* **2015**, *9*, 12. (b) Shiraishi, N.; Inai, Y.; Bi, W. M.; Nishikimi, M. Fragmentation and dimerization of copper-loaded prion protein by copper-catalysed oxidation. *Biochem. J.* **2005**, *387*, 247−255.

(22) (a) Ciregna, D.; Monzani, E.; Thiabaud, G.; Pizzocaro, S.; Casella, L. Copper-β-amyloid peptides exhibit neither monooxygenase nor superoxide dismutase activities. *Chem. Commun.* **2013**, *49*, 4027−4029. (b) Pirota, V.; Dell'Acqua, S.; Monzani, E.; Nicolis, S.; Casella, L. Copper-Aβ peptides and oxidation of catecholic substrates: Reactivity and endogenous peptide damage. *Chem. - Eur. J.* **2016**, *22*, 16964−16973.

(23) (a) Dell'Acqua, S.; Pirota, V.; Anzani, C.; Rocco, M. M.; Nicolis, S.; Valensin, D.; Monzani, E.; Casella, L. Reactivity of copper-α-synuclein peptide complexes relevant to Parkinson's disease. *Metallomics* **2015**, *7*, 1091−1102. (b) Dell'Acqua, S.; Pirota, V.; Monzani, E.; Camponeschi, F.; De Ricco, R.; Valensin, D.; Casella, L. Copper(I) forms a redox-stable 1:2 complex with α-synuclein N-terminal peptide in a membrane-like environment. *Inorg. Chem.* **2016**, *55*, 6100−6106.

(24) Herlinger, E.; Jameson, R. F.; Linert, W. Spontaneous autoxidation of dopamine. *J. Chem. Soc., Perkin Trans. 2* **1995**, 259−263.

(25) Di Natale, G.; Grasso, G.; Impellizzeri, G.; La Mendola, D.; Micera, G.; Mihala, N.; Nagy, Z.; Osz, K.; Pappalardo, G.; Rigo, V.; Rizzarelli, E.; Sanna, D.; Sovago, I. Copper(II) interaction with unstructured prion domain outside the octarepeat region: Speciation, stability, and binding details of copper(II) complexes with PrP106−126 peptides. *Inorg. Chem.* **2005**, *44*, 7214−7225.

(26) (a) Pham, A. N.; Waite, T. D. Cu(II)-catalyzed oxidation of dopamine in aqueous solutions: Mechanism and kinetics. *J. Inorg. Biochem.* **2014**, *137*, 74−84. (b) Nemeikaite-Ceniene, A.; Imbrasaite, A.; Sergediene, E.; Cenas, N. Quantitative structure-activity relationships in prooxidant cytotoxicity of polyphenols: role of potential of phenoxyl radical/phenol redox couple. *Arch. Biochem. Biophys.* **2005**, *441*, 182−190.

(27) Davies, P.; Marken, F.; Salter, S.; Brown, D. R. Thermodynamic and voltammetric characterization of the metal binding to the prion protein: Insights into pH dependence and redox chemistry. *Biochemistry* **2009**, *48*, 2610−2619.

(28) Valensin, D.; Dell'Acqua, S.; Kozlowski, H.; Casella, L. Coordination and redox properties of copper interaction with α-synuclein. *J. Inorg. Biochem.* **2016**, *163*, 292−300.

(29) (a) Liu, L.; Jiang, D.; mcdonald, A.; Hao, Y.; Millhauser, G. L.; Zhou, F. Copper redox cycling in the prion protein depends critically on binding mode. *J. Am. Chem. Soc.* **2011**, *133*, 12229−12237. (b) Arcos-Lopez, T.; Qayyum, M.; Rivillas-Acevedo, L.; Miotto, M. C.; Grande-Aztatzi, R.; Fernandez, C. O.; Hedman, B.; Hodgson, K. O.; Vela, A.; Solomon, E. I.; Quintanar, L. Spectroscopic and theoretical study of cu^{i} binding to His111 in the human prion protein fragment 106−115. *Inorg. Chem.* **2016**, *55*, 2909−2922.

(30) Cassagnes, L.-E.; Hervé, V.; Nepveu, F.; Hureau, C.; Faller, P.; Collin, F. The Catalytically active copper-amyloid-beta state: Coordination site responsible for reactive oxygen species production. *Angew. Chem., Int. Ed.* **2013**, *52*, 11110−11113.

(31) Solomon, E. I.; Heppner, D. E.; Johnston, E. M.; Ginsbach, J. W.; Cirera, J.; Qayyum, M.; Kieber-Emmons, M. T.; Kjaergaard, C. H.; Hadt, R. G.; Tian, L. Copper active sites in biology. *Chem. Rev.* **2014**, *114*, 3659−3853.

(32) Grubman, A.; White, A. R. Copper as a key regulator of cell signalling pathways. *Expert Rev. Mol. Med.* **2014**, *16*, e11.

(33) (a) Conway, K. A.; Rochet, J. C.; Bieganski, R. M.; Lansbury, P. T., Jr. Kinetic stabilization of the alpha-synuclein protofibril by a dopamine-alpha-synuclein adduct. *Science* **2001**, *294*, 1346−1349. (b) Bisaglia, M.; Mammi, S.; Bubacco, L. Kinetic and structural analysis of the early oxidation products of dopamine. *J. Biol. Chem.* **2007**, *282*, 15597−15605.

(34) Lavoie, M. J.; Ostaszewski, B. L.; Weihofen, A.; Schlossmacher, M. G.; Selkoe, D. J. Dopamine covalently modifies and functionally inactivates parkin. *Nat. Med.* **2005**, *11*, 1214−1221.

(35) Nobili, A.; Latagliata, E. C.; Viscomi, M. T.; Cavallucci, V.; Cutuli, D.; Giacovazzo, G.; Krashia, P.; Rizzo, F. R.; Marino, R.; Federici, M.; De Bartolo, P.; Aversa, D.; Dell'Acqua, M. C.; Cordella, A.; Sancandi, M.; Keller, F.; Petrosini, L.; Puglisi-Allegra, S.; Mercuri, N. B.; Coccurello, R.; Berretta, N.; D'Amelio, M. Dopamine neuronal loss contributes to memory and reward dysfunction in a model of Alzheimer's disease. *Nat. Commun.* **2017**, *8*, 14727.

(36) (a) McDonald, A. J.; Dibble, J. P.; Evans, E. G. B.; Millhauser, G. L. A new *paradigm* for enzymatic control of α-cleavage and β-cleavage of the prion protein. *J. Biol. Chem.* **2014**, *289*, 803−813. (b) Watt, N. T.; Taylor, D. R.; Gillott, A.; Thomas, D. A.; Perera, W. S.; Hooper, N. M. Reactive oxygen species-mediated β-cleavage of the prion protein in the cellular response to oxidative stress. *J. Biol. Chem.* **2005**, *280*, 35914−35921.

(37) Zucca, F. A.; Segura-Aguilar, J.; Ferrari, E.; Munoz, P.; Paris, I.; Sulzer, D.; Sarna, T.; Casella, L.; Zecca, L. Interactions of iron, dopamine and neuromelanin pathways in brain aging and Parkinson's disease. *Prog. Neurobiol.* **2015**, http://dx.doi.org/10.1016/j.pneurobio.2015.09.012.*1559*610.1016/j.pneurobio.2015.09.012

(38) (a) Zecca, L.; Bellei, C.; Costi, P.; Albertini, A.; Monzani, E.; Casella, L.; Gallorini, M.; Bergamaschi, L.; Moscatelli, A.; Turro, N. J.; Eisner, M.; Crippa, P. R.; Ito, S.; Wakamatsu, K.; Bush, W. D.; Ward, W. C.; Simon, J. D.; Zucca, F. A. New melanic pigments in the human brain that accumulate in aging and block environmental toxic metals. *Proc. Natl. Acad. Sci. U. S. A.* **2008**, *105*, 17567−17572. (b) Engelen, M.; Vanna, R.; Bellei, C.; Zucca, F. A.; Wakamatsu, K.; Monzani, E.; Ito, S.; Casella, L.; Zecca, L. Neuromelanins of human brain have soluble and insoluble components with dolichols attached to the melanic structure. *PLoS One* **2012**, *7*, e48490.

(39) Kawahara, M.; Kato-Negishi, M.; Tanaka, K. Cross talk between neurometals and amyloidogenic proteins at the synapse and the pathogenesis of neurodegenerative diseases. *Metallomics* **2017**, *9*, 619.

(40) Monzani, E.; Quinti, L.; Perotti, A.; Casella, L.; Gullotti, M.; Randaccio, L.; Geremia, S.; Nardin, G.; Faleschini, P.; Tabbì, G. Tyrosinase models. Synthesis, structure, catechol oxidase activity, and phenol monooxygenase activity of a dinuclear copper complex derived from a triamino pentabenzimidazole ligand. *Inorg. Chem.* **1998**, *37*, 553−562.

(41) Alderighi, L.; Gans, P.; Ienco, A.; Peters, D.; Sabatini, A.; Vacca, A. Hyperquad simulation and speciation (HYSS): a utility program for the investigation of equilibria involving soluble and partially soluble species. *Coord. Chem. Rev.* **1999**, *184*, 311−318.

(42) Arena, G.; Cali, R.; Rizzarelli, E.; Sammartano, S. Thermodynamic study on the formation of the cupric ion hydrolytic species. *Thermochim. Acta* **1976**, *16*, 315−321.

DOI: 10.1021/acs.inorgchem.7b01757
Inorg. Chem. 2017, 56, 11317−11325

(43) Sokołowska, M.; Bal, W. Cu(II) complexation by "non-coordinating" N-2-hydroxyethylpiperazine-N′-2-ethanesulfonic acid (HEPES buffer). *J. Inorg. Biochem.* **2005**, *99*, 1653−1660.
(44) Bielski, B. H. J.; Shiue, G. G.; Bajuk, S. Reduction of nitro blue tetrazolium by CO_2^- and O_2^- radicals. *J. Phys. Chem.* **1980**, *84*, 830−833.

DOI: 10.1021/acs.inorgchem.7b01757
Inorg. Chem. 2017, 56, 11317−11325